Full Paper: The phase morphology and rheological properties of a series of poly(methyl methacrylate)-*block*-poly(isooctyl acrylate)-*block*-poly(methyl methacrylate) triblock copolymers (MIM) have been studied. These copolymers have well-defined molecular structures, with a molecular weight (MW) of poly(methyl methacrylate) (PMMA) in the range of 3500–50000 and MW of poly(isooctyl acrylate) (PIOA) ranging from 100000 to 140000. Atomic force microscopy with phase detection imaging has shown a two-phase morphology for all the MIM copolymers. The typical spherical, cylindrical, and lamellar phase morphologies have been observed depending on the copolymer composition. MIM consisting of very short PMMA end blocks (MW 3500–5000) behave as thermoplastic elastomers (TPEs), with however an upper-service temperature higher than the traditional polystyrene-*block*-polyisoprene-*block*-polystyrene TPEs (Kraton D1107). A higher processing temperature is also noted, consistent with the higher viscosity of PMMA compared to PS.

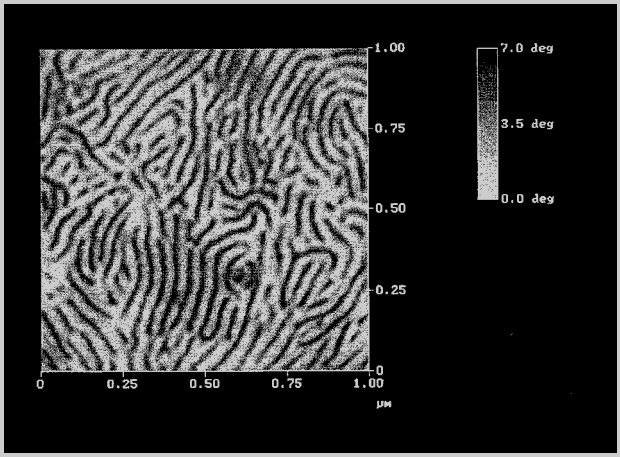

Phase detection image for MIM triblocks: (b) cylindrical morphology for sample 5

Morphology and rheology of poly(methyl methacrylate)-*block*-poly(isooctyl acrylate)-*block*-poly(methyl methacrylate) triblock copolymers, and potential as thermoplastic elastomers

J. D. Tong[1], *Ph. Leclère*[2], *A. Rasmont*[2], *J. L. Brédas*[2], *R. Lazzaroni*[2], *R. Jérôme**[1]

[1] Center for Education and Research on Macromolecules (CERM), University of Liège, Sart-Tilman B6, 4000 Liège, Belgium
[2] Service de Chimie des Matériaux Nouveaux, Centre de Recherche en Electronique et Photonique Moléculaires, Université de Mons-Hainaut, Place du Parc 20, 7000 Mons, Belgium

(Received: March 8, 1999; revised: July 2, 1999)

Introduction

Recent developments in ligated anionic polymerization[1)] of acrylic monomers have led to the controlled synthesis of new block copolymers, such as poly(methyl methacrylate)-*block*-poly(alkyl acrylate)-*block*-poly(methyl methacrylate)[2)] (MAM) and poly(alkyl methacrylate)-*block*-polybutadiene-*block*-poly(alkyl methacrylate)[3)] triblocks. These new materials have the potential of replacing advantageously the traditional styrene-diene based thermoplastic elastomers (TPEs), whose the practical use is limited by the poor oxidation resistance of the central polydiene block and by the low service temperature (60∼70 °C) dictated by to the glass transition temperature (T_g) of the outer polystyrene (PS) blocks.

Interest for fully acrylic triblock copolymers, thus consisting of inner soft polyacrylate block and outer hard polymethacrylate blocks, has to be found in the wide range of properties that can be made available merely by changing the alkyl substituent of the ester group. For instance, T_g can span a large range from −50 °C for poly(isooctyl acrylate) (PIOA) up to 190 °C for poly(isobornyl methacrylate). Furthermore, immiscibility of poly(methyl methacrylate) (PMMA) and poly(alkyl acrylates) is the rule, although some exceptions may be found in the case of small alkyl groups and low molecular weight[4)]. The much better resistance of acrylic polymers to UV and oxidation compared to polydienes is clearly beneficial. A previous paper has reported on the controlled synthesis

  1022-1352/2000/1208–1250$17.50+.50/0

and mechanical properties of PMMA-*block*-PIOA-*block*-PMMA triblock copolymers (MIM)[5]. The phase morphology and the rheological properties of these MIM triblock copolymers have been analyzed further and are the topic of this paper.

Experimental part

Materials

MIM triblock and MI diblock copolymers were synthesized by sequential anionic polymerization of MMA, *tert*-butyl acrylate (tBA) (and MMA, in case of triblocks) respectively, followed by the acid-catalyzed transalcoholysis of the *tert*-butyl ester groups by isooctyl alcohol. The detailed synthesis was reported elsewhere[2,5]. The molecular characteristics of the MIM triblocks and the MI diblock are listed in Tab. 1. A commercial grade polystyrene-*block*-polyisoprene(PIP)-*block*-polystyrene triblock copolymer, SIPS (Kraton D1107 from Shell Development Company, 15∼18 wt.-% uncoupled diblock), was used for the sake of comparison. The announced molecular weight (MW) was 10000–120000–10000, with a polystyrene content of 15 wt.-%.

Sample preparation

Thin MIM films were cast on mica from dilute solution in THF (2 mg/ml) and sheltered from dust throughout. THF was let to evaporate very slowly for a few days. The films were annealed at 140 °C under high vacuum for 24 h before AFM observation. The film thickness was ca. 500 nm. Longer annealing times and longer thickness did not change the microphase morphology. Some topological defects were however observed for 1–2 mm thick samples. Films suited to rheological testing, were prepared by casting a copolymer solution (8 wt.-%; 160 ml) in a 100 mm diameter polyethylene dish. The solvent was evaporated over 4 days at room temperature. Ca. 1.5 mm films were dried to constant weight in a vacuum oven at 80 °C for ca. 1 day. The reason for milder conditions compared to the preparation of films for AFM observation must be found in the possible dehydration at 140 °C of the residual carboxylic acids left by the transalcoholysis reaction, which might affect the rheological data in contrast to the already set up phase morphology. Accordingly, rheology will not be discussed in direct relation to the microphase morphology observed by AFM. The specimens were colorless, transparent and elastomeric with a smooth surface.

AFM observation

All the AFM images were recorded with a Nanoscope IIIa microscope from Digital Instruments Inc. operated in the Tapping Mode (at 25 °C, in air). Microfabricated cantilevers were used with a spring constant of 30 $N \cdot m^{-1}$. The instrument is equipped with the Extender TM Electronics Module, such that height and phase cartographies can be simultaneously recorded. Several areas of the same sample were observed, with scanning time of ca. 5 min. The phase image was recorded in the so-called "soft tapping mode"[6] in order to avoid deformation and indentation of the polymer surface by the tip. All the images were recorded with the maximum available number of pixels (512) in each direction. For image analysis, the Nanoscope image processing software was used. The images were usually reported as captured, repeated scans assessing the reproducibility of the observed structures.

Rheological measurements

The RSI ARES rheometer from Rheometrics equipped with a force balance transducer was used, either in the cone-plate mode: (plate: 25 mm diameter, cone: 4° angle, gap: 56 μm between the cone tip and the plate; for samples 1 and 7) or in the parallel plate mode (25 mm diameter, for all the other samples). The temperature control was better than 1 °C. The applied strain was always kept within the linear viscoelastic regime, so that the phase morphology did not change under shearing. The frequency range was between 0.1 Hz∼16.7 Hz. A Polymer Laboratory DMTA (parallel plate with 7 mm diameter) was used to conduct temperature sweep experiments at 1 Hz (ramp mode, heating rate of 2 °C/min).

Results and discussion

Phase morphology

The very low electronic contrast between the constitutive blocks of poly alkyl(meth)acrylate-containing triblocks is quite a problem for the observation of nanophase-separated morphology by transmission electron microscopy (TEM) and small angle X-ray scattering (SAXS). Only indirect techniques, such as NMR[7] and DMTA[5], have been used for this purpose. However, atomic force microscopy (AFM) with phase detection imaging has proved very recently to be very appropriate to the direct observation of phase separation in fully acrylic block copolymers[8]. In this work, tapping-mode atomic force microscopy (TMAFM) with phase detection imaging (PDI) has been used, this technique having proven high efficiency for the analysis of the phase morphology of polystyrene-*block*-polyisoprene-*block*-polystyrene copolymers[9].

Fig. 1 shows typical AFM images for the MIM triblock containing 6.5 wt% PMMA (sample 1, Tab. 1). The height image (Fig. 1a) is very uniform, thus indicating that the sample surface is very smooth, in line with ca. 1.4 nm root mean square roughness for a $1 \times 1\ \mu m^2$ area. This preliminary observation is a guarantee that any contrast observed in the PDI image will not originate from differences in the surface topography. The phase image (Fig. 1b) clearly shows a two-phase morphology for the sample 1, that consists of bright spheres randomly distributed in a dark matrix. Recent models proposed[10] to account for the phase contrast in TMAFM indicate that in "soft tapping" operation, the phase shift is directly related

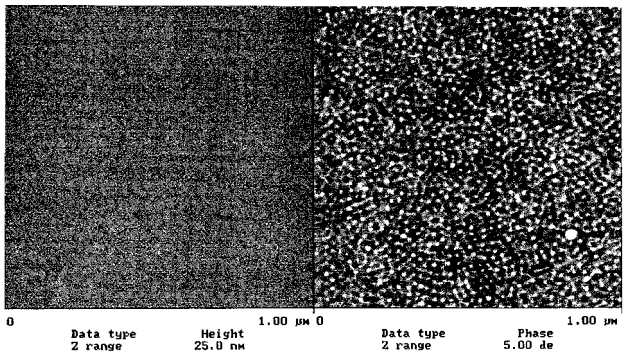

Fig. 1. Tapping mode AFM image for MIM triblock (sample 1, Tab. 1): (a) height image; (b) phase image

to the Young's modulus of the probed material. The bright spots can accordingly be assigned to PMMA, which is harder than PIOA, so resulting in a larger phase shift. A close look at the image (Fig. 1b) shows that the cross-sectional area of the white spheres exceeds the value expected from the actual composition (6.5 wt.-%). The

Tab. 1. Molecular characteristics of MIM triblock and MI diblock copolymers

Sample	Molecular weight $\overline{M}_n$ in g/mol × 10^{-3}	$\overline{M}_w/\overline{M}_n$	Content of PMMA in wt.-%
1	3.5–100–3.5	1.04	6.5
2	5–140–5	1.06	6.6
3	7–100–7	1.07	12.2
4	10–140–10	1.05	12.5
5	20–140–20	1.04	22.2
6	40–140–40	1.06	36.4
7	50–140–50	1.06	41.6
8	10–140	1.04	6.7
9	83 wt.-% sample 4 + 17 wt.-% sample 8	–	11.5

origin of this apparent disagreement has to be found in the apex radius of the AFM tip (ca. 20 nm), which is close to the sphere diameter (15∼20 nm). This relatively large tip contributes to the broadening of the domain/matrix boundary, so preventing the sphere diameter from being quantitatively measured. From the Fourier analysis of the AFM data, the periodicity of the phase morphology can be calculated, the center-to-center distance between the near-neighboring spheres being 27 nm.

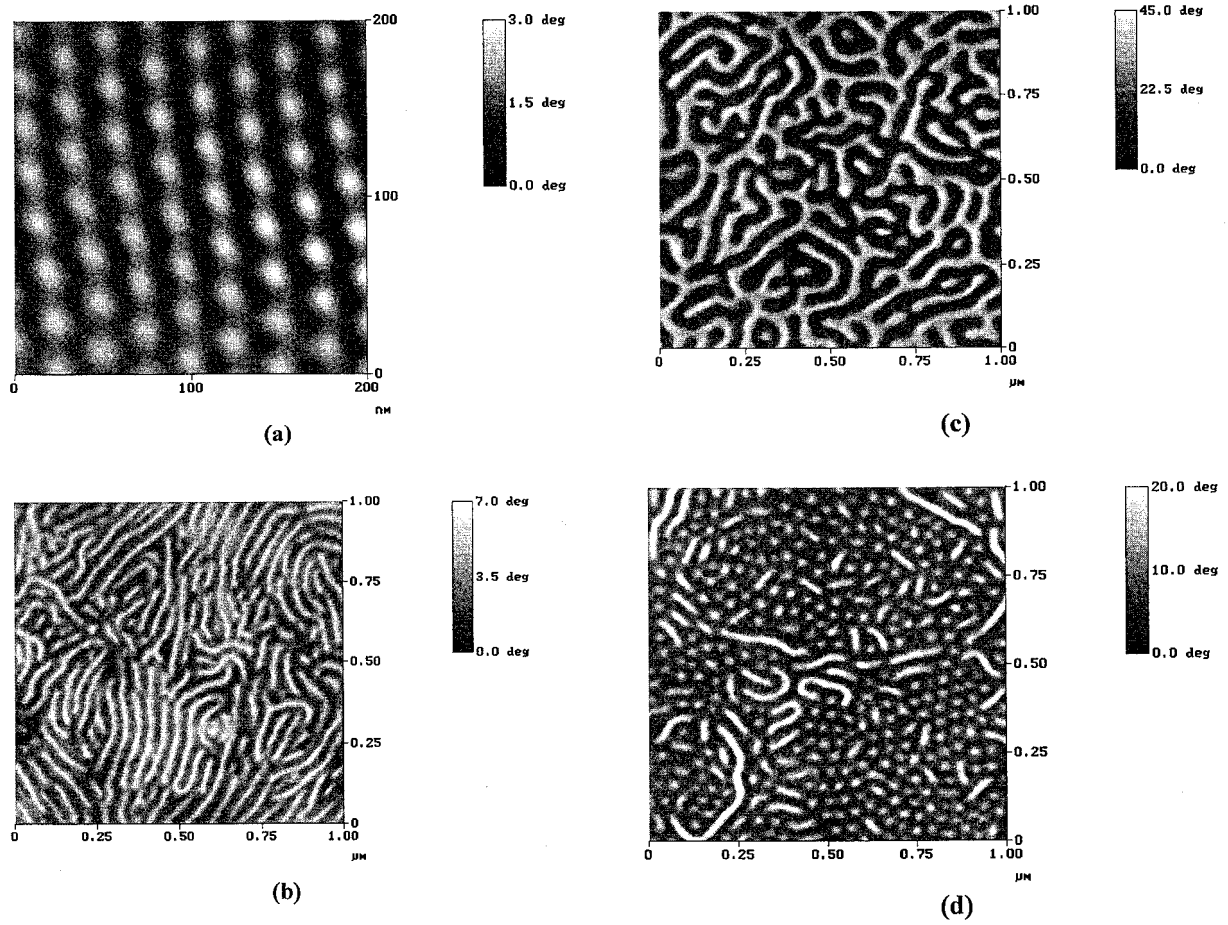

Fig. 2. Phase detection image for MIM triblocks: (a) spherical morphology for sample 3; (b) cylindrical morphology for sample 5; (c) lamellar morphology for sample 6; (d) cylindrical morphology for sample 5 after annealing at 140 °C for 24 h

The equilibrium phase morphology of block copolymers strongly depends on the copolymer composition, as illustrated by the styrene-diene block copolymers[11, 12]. Spherical morphology is commonly observed for polystyrene (PS) contents up to ~17 wt%. When the PS content ranges from 17 to 38 wt.-%, the phase morphology is cylindrical, whereas a lamellar morphology is reported for 36~62 wt.-% PS. For the sake of comparison, a series of MIM copolymers covering a wide range of PMMA composition has been analyzed by AFM. Fig. 2 shows some typical phase morphologies: PMMA spheres (Fig. 2a) for sample 3 of low PMMA content (12 wt.-%), PMMA cylinders (Fig. 2b) for sample 5 of intermediate PMMA content (22 wt.-%), and PMMA short lamellae (Fig. 2c) for sample 6 of higher PMMA content (36 wt.-%). Although the copolymer composition-phase morphology relationship is basically comparable for MIM and styrene-diene block copolymers, MIM with very short PMMA blocks ($\overline{M}_n$: 3500) shows a well-defined spherical morphology, in contrast to the PS-*block*-polybutadiene (PB)-*b*-PS (SBS) and SIPS analogues[13] that show no phase separation.

The annealing of sample 5 has a strong effect on the orientation of the PMMA cylinders with respect to the sample surface. Before annealing, the cylinders lie flat on the surface (Fig. 2b). After annealing at 140 °C, only a few flat cylinders coexist with many bright dots whose diameter is similar to the width of the flat cylinders. This observation is consistent with the fact that the bright dots are cylinders standing upright perpendicular to the surface (Fig. 2d). This reorganization is likely to be governed by the surface energy, which is smaller for PIOA (30×10^{-3} N/m) than for PMMA (41×10^{-3} N/m). As the equilibrium is approached, the PMMA cylinders tend to reorganize themselves with their apex at the surface.

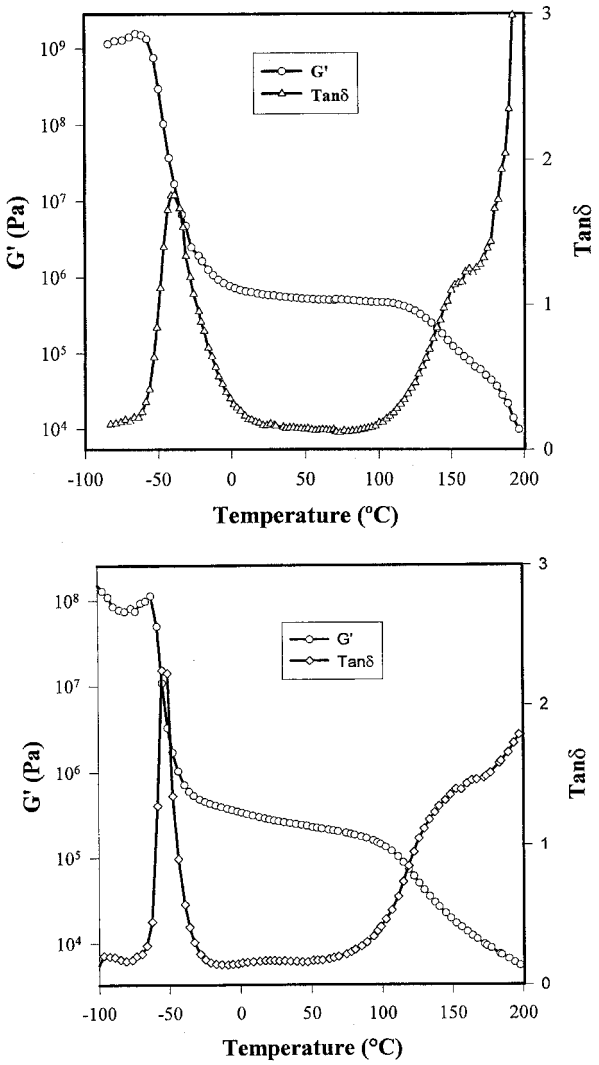

Fig. 3. Temperature dependence of the shear storage modulus (G') and the loss factor (tanδ) (1 Hz, heating rate: 2 °C/m). (a) MIM triblock, sample 2; (b) Kraton D1107

Viscoelastic behavior of MIM triblock copolymers

It is well established that the domain structure of block copolymers, such as SBS and SIPS, persists beyond the upper (PS) glass transition temperature. However, as temperature is raised above a critical value, the microdomain structure disappears completely, resulting in a homogeneous system. This transition is referred to as the order-disorder transition (ODT), which occurs in all known block copolymers[14–18]. The viscoelastic behavior of these block copolymers significantly changes at the ODT, the block copolymer being easily processable beyond ODT.

Dynamic temperature sweep experiments

Fig. 3 compares the temperature dependence of the storage modulus (G') and the loss factor (tanδ) measured at 1 Hz for the 5000–140000–5000 MIM triblock (sample 2, Tab. 1) and the Kraton D1107 sample. The dynamic mechanical behavior of these samples is typical of thermoplastic elastomers, i.e. two transitions, a rubbery plateau between them and the terminal zone at higher temperature. Compared to Kraton D1107, the MIM sample (Fig. 3a) has quite a comparable behavior, except for the G' plateau region which is more flat (up to 110 °C) as result of the absence of diblock copolymers[19]. The tanδ curves do not exhibit any clear peak at the T_g of PS (or PMMA) microdomains, which can be explained by the low PS (or PMMA) content and the simultaneous occurrence of the flow.

Fig. 4 compares the logG' vs. temperature curves for a series of MIM triblock copolymers covering a large range of PMMA molecular weight (3500–20000). The behavior of MIM triblocks is similar to that of the Kraton TPE when the PMMA molecular weight is smaller than 7000. However, when this molecular weight is higher, no terminal zone is observed up to 200 °C, the highest tempera-

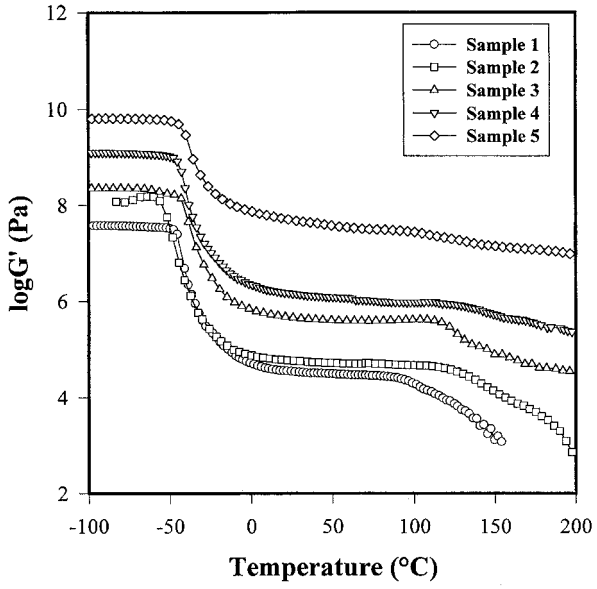

Fig. 4. Temperature dependence of the shear storage modulus (G') for a series of MIM triblocks at 1 Hz (heating rate: 2 °C/m). For the sake of clarity, curves have been vertically shifted with respect to sample 2 (sample 1 downwards by 0.5 unit; samples 3, 4 and 5, upwards by 0.5, 1.0 and 1.5 units, respectively

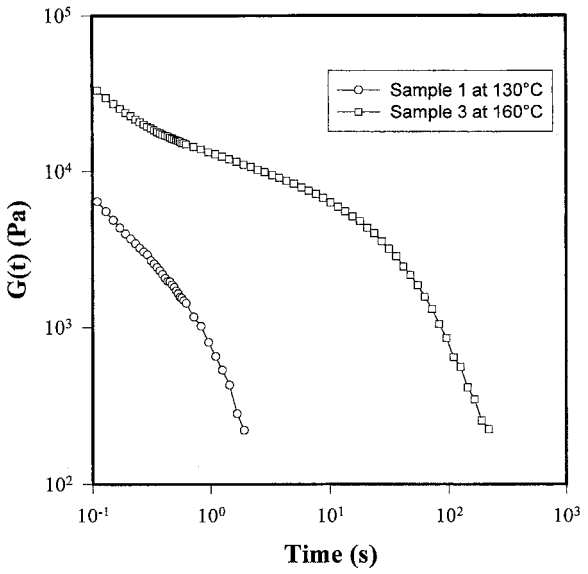

Fig. 5. Time dependence of the stress modulus for two MIM triblocks (samples 1 and 3, in Tab. 1)

ture tested. It is known that G' measured at low frequencies decreases sharply at or near the order-disorder transition temperature (T_{ODT}) of the block copolymer[20–23]. It is thus obvious that a phase-separated morphology persists beyond the glass transition of the PMMA microdomains of samples 3 to 5, at least up to 200 °C. The comparison of MIM and SIPS of comparable molecular structure (sample 4 and Kraton D1107), also shows that G' starts to decrease only at 120 °C for MIM, which is ca. 20 °C higher than for the SIPS sample, in agreement with a higher service temperature for the MIM triblock copolymer.

Relaxation at temperatures beyond T_g of PMMA

The rheological properties of polymers are closely related to the relaxation process of the polymer chains. Recently, Berglund and McKay have thoroughly studied the relaxation behavior of SIPS triblock copolymers[19]. The complete relaxation stress proceeds in two steps: diffusion of the outer blocks out of the microdomains, followed by diffusion of the released chains through the entangled midblock chains. Fig. 5 compares the relaxation for two MIM triblocks of different PMMA molecular weight (samples 1 and 3) but of the same spherical morphology. The relaxation curve for the MIM containing PMMA blocks of 7000 MW clearly confirms Berglund and McKay's conclusion, i.e. a two-step drop of $G(t)$ in the $10^{-1} \sim 10^{1}$ s and $10^{1} \sim 2 \times 10^{2}$ s regions, respectively, assigned to the relaxation of the PMMA blocks out of the hard microdomains followed by the diffusion of the entire chains through the PIOA matrix. The relaxation of MIM containing two times shorter PMMA blocks is quite reminiscent of that one commonly observed for monophase polymers, so indicating that no microdomain structure persists at 130 °C.

Dynamic frequency sweep experiments

Fig. 6 illustrates how the complex viscosity of sample 2 depends on the angular frequency. The complex viscosity at 120 °C is clearly non-Newtonian, as is the case for vulcanized rubber. A yield behavior starts to be observed at 180 °C, and a Newtonian behavior at low shear rate, as well. The observation that the Newtonian behavior becomes more pronounced as the temperature is increased beyond some limit, is the signature of the complete relaxation of the triblock chains at low angular frequency when T_{ODT} of the block copolymer is approached[19]. Fig. 7 compares the plots of complex viscosity vs. angular frequency for a series of MIM triblocks at 170 °C. As the PMMA molecular weight is increased, the non-Newtonian behavior is continuously more pronounced, as a result of increasingly more extended phase separation when the molecular weight[24] is increased.

Fig. 8 compares the complex viscosity of MIM/MI binary blend (sample 9, Tab. 1) and Kraton D1107. It must be noted that although the MIM/MI binary blend contains the same diblock content as the Kraton copolymer, the content of the hard block (ca. 11.5 wt.-%) is smaller compared to Kraton (ca. 15 wt.-%). Moreover, the molecular weight between chain entanglements (M_e) is 60000 for PIOA[6] much higher than the 6100 for PIP[2]. For these

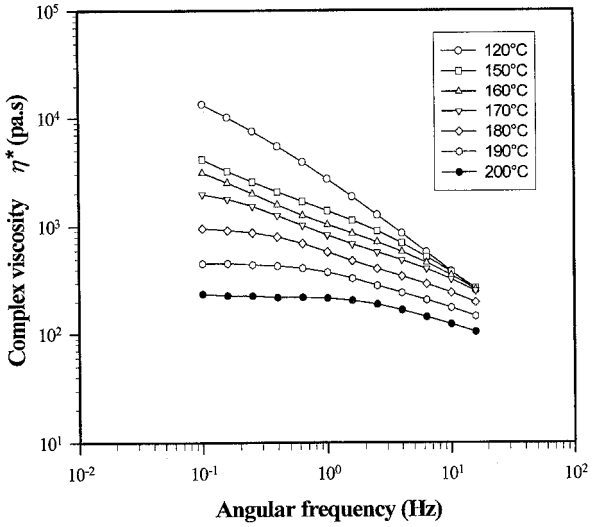

Fig. 6. Plots of complex viscosity vs. angular frequency for the MIM sample 2

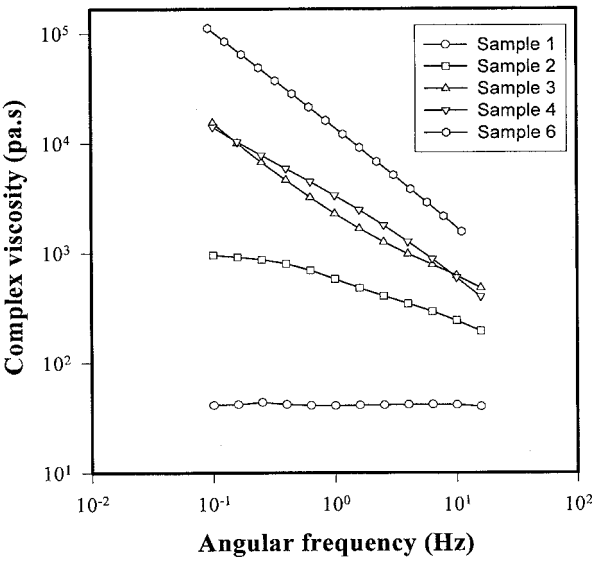

Fig. 7. Plots of complex viscosity vs. angular frequency for a series of MIM triblocks (Tab. 1) at 180 °C

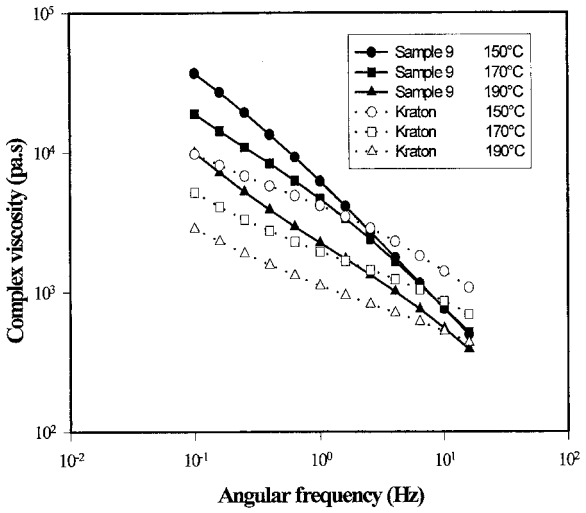

Fig. 8. Plots of complex viscosity vs. angular frequency for the MIM/MI binary blend (sample 9, open symbols) and Kraton D1107 (filled symbols)

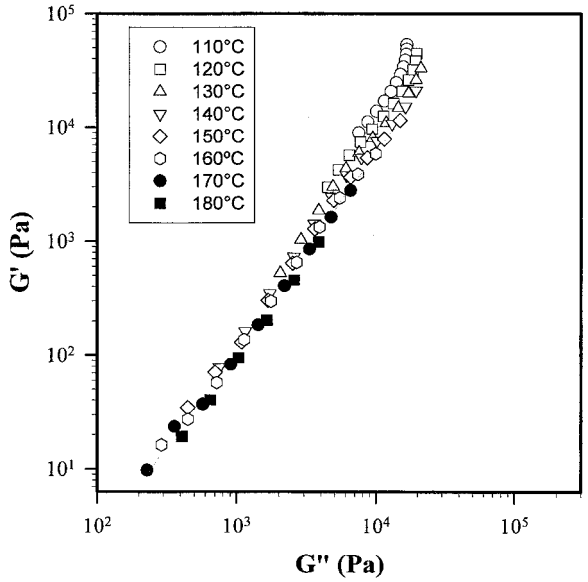

Fig. 9. $\log G'$ vs. $\log G''$ for the MIM sample 1. The slope is 2 at 170 °C and 180 °C

two reasons, not only the shear modulus but also the complex viscosity are expected to be higher for the Kraton copolymer than for the MIM/MI counterpart. This expectation is confirmed for the complex viscosity at 150 °C at high shear rates. However, as the temperature is increased, the complex viscosity of sample 9 remains higher compared to the Kraton sample in a larger range of shear rates, indicating more restricted relaxation and better persistence of the microdomain structures for the MIM copolymer at high temperatures.

Order-disorder transition temperature

As long as the microdomains persist beyond T_g of PMMA, they contribute to keeping the melt viscosity high[26], which is undesirable for the processing of the MIM copolymers. Han and co-workers[27] have recently shown that rheological data can be used to determine the order-disorder transition temperature, as illustrated in Fig. 9, where $\log G'$ is plotted vs. $\log G''$ at different temperatures. According to these authors, the threshold temperature at which the $\log G'$ vs. $\log G''$ plot becomes linear and the slope (of 2) becomes independent of temperature is the signature of the order-disorder transition. This prediction is based on a rheological model suited to homogeneous polymers in the terminal zone (Eq. (1)):

$$\log G' = 2 \log G'' - \log(\rho RT/M_e) + \log(\pi^2/8) \qquad (1)$$

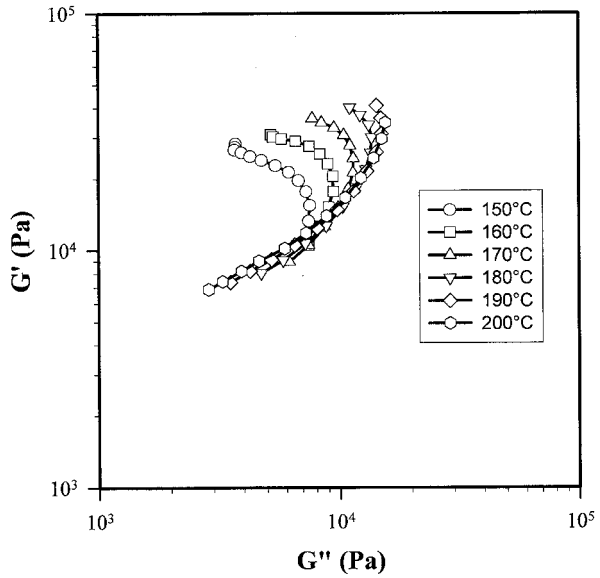

Fig. 10. $\log G'$ vs. $\log G''$ for the MIM sample 4

Tab. 2. T_{ODT} for MIM and SIS block copolymers[a)]

Sample	$\bar{M}_n \times 10^{-3}$	Content of hard block in wt.-%	T_{ODT}/°C
SIS-1[28)]	7.4–99–7.4	11.4	180
SIS-2[19)]	10.6–125.4–10.6	14.5	280
Kraton D1107[27)]	10–120–10 + (15∼18% diblock)	14.3	230
MIM-1	3.5–100–3.5	6.5	130–140
MIM-2	5–140–5	6.6	200
MIM-3	7–100–7	12.2	>200
MIM-4	10–140–10	12.5	>200
MIM-9	10–140–10 + (17% diblock)	11.5	>200

[a)] Measured by Han's method[18)].

where ρ is the polymer density, R the gas constant, T the absolute temperature and M_e the molecular weight between chain entanglements. Fig. 9 shows that plots of $\log G'$ vs. $\log G''$ for the MIM sample 1 (Tab. 1) are not linear (data collected from frequency sweep experiments) below 130–140 °C, particularly at higher frequency (upper part of the curves). As the temperature exceeds 130–140 °C, the $\log G'$ vs. $\log G''$ curve is linear with a slope of 2, so indicating that T_{ODT} lies in this temperature range, at least in the range of the investigated frequencies (0.1∼15.9 Hz). Fig. 10 illustrates the same relationship for the MIM sample 4, which contains more PMMA (12 wt.-%) of higher molecular weight (7000) although preserving the same spherical morphology. Plots of $\log G'$ vs. $\log G''$ are far from linearity and superposition, indicating that T_{ODT} is well beyond the range of the investigated temperatures (150–200 °C). Tab. 2 lists the values of T_{ODT}, as determined by Han's method for a series of MIM triblocks. Data for SIPS copolymers are also reported from the scientific literature[19, 27, 28)]. It is clear that the T_{ODT} of MIM triblocks is much higher than T_{ODT} of the SIPS analogues, this might be a problem for the copolymer processing, since the degradation temperature of the polyacrylate central block is only 230 °C as measured by TGA (5 °/min, N_2).

Viscoelastic properties of polystyrene and poly(methyl methacrylate) homopolymers

The origin of the difference in T_{ODT} of MIM and SIPS copolymers might be found in the polymer-polymer interaction parameter, χ_{ab}, for the PMMA/PIOA and the PS/PIP pairs. The χ_{ab} value is commonly determined from the solubility parameter for each component at constant molecular weight[24)]:

$$\chi_{ab} = M_a(\delta_a - \delta_b)^2/\rho_a RT$$

where M_a the is molecular weight of component a; δ_a and δ_b are the solubility parameters of components a and b; ρ_a is the density of component a. The solubility parameters for PMMA, poly(alkyl acrylates) (e.g. ethyl, propyl, butyl), PS, and PIP are 18.6, 18.0∼19.8, 19.0, and 16∼17 $(J/cm^3)^{1/2}$ [29)] respectively. Thus, $\delta_a - \delta_b$ for the PMMA/PIOA pair is expected to be smaller than for the PS/PIP pair, although the exact value of δ for PIOA is unknown. The smaller polymer-polymer interaction parameter for the PMMA/PIOA pair compared to the PS/PIP pair is thus in favor of a lower degree of immiscibility and thus a lower order-disorder transition temperature for the MIM copolymers, which completely disagrees with the experimental observations.

The physico-mechanical characteristics of the hard blocks may not be ignored when the melt processing of the triblock TPEs are concerned. Although the volume and molecular weight of the monomer units and T_g are comparable for PMMA and PS, these two polymers have quite a different behavior in solution and in the melt. For example, Tab. 3 shows that M_e for PS is roughly three times as large as M_e for PMMA and that the viscoelastic coefficients extracted from the WLF equation are also different[30–35)]. The viscoelastic characteristics for PMMA and PS (Tab. 3) have been reported for samples prepared by free-radical polymerization, thus for samples of very broad molecular weight distribution, which might explain the dispersion of some rheological properties depending on their origin. In order to improve the accuracy of the M_e values, PMMA ($\bar{M}_n$: 5000 to 80000) and PS ($\bar{M}_n$: 10000) homopolymers have been prepared, in this study, by anionic polymerization, so making samples of very narrow molecular weight distribution (<1.1) available. M_e for PMMA has been found to be 6000, consistent with the previously reported data[30)]. Tab. 4 provides the zero-

Tab. 3. Viscoelastic characteristics for PMMA and PS[a)]

Sample	$G_N^0 \times 10^5$ / Pa	M_e / g/mol	M_c [b)] / g/mol	C_1[c)]	C_2[c)] / °C
PMMA	6.57	4700~9200	17600~27500	9.0	13.4
PS	1.99	17300~18700	31200~32800	35.5	55

a) Data from refs.[30–35)]

b) Critical molecular weight at which the molecular weight (M) dependence of η_0 changes from $\eta_0 = KM$ ($M < Mc$) to $\eta_0 = K'M^{3.4}$ ($M > Mc$). η_0 is the zero-shear viscosity defined as $\eta_0 = \lim_{\omega \to 0} (G''/\omega)$, with ω the shear rate and G'' the shear loss modulus.

c) Coefficients of the WLF equation, $-\log a_T = C_1 (T-T_0)/(C_2 + T-T_0)$

Tab. 4. Zero-shear viscosity for PMMA and PS at 170 °C

Sample	$\overline{M}_n$ and ($\overline{M}_w/\overline{M}_n$)	η_0/(Pa · s)
PMMA	5000 (1.10)	1800
PMMA	8000 (1.07)	3700
PMMA	10000 (1.05)	7000
PMMA	20000 (1.04)	80000[a)]
PS	10000 (1.10)	44
PS	48500 (1.10)	1500[b)]

a) 180 °C.

b) 183 °C[36)].

shear viscosity (η_0) measured at 170 °C for these PMMA and PS samples. The experimental viscosity for PMMA of 10000 MW is more than 150 times larger compared to PS of the same MW. Even when the PMMA MW is half that of the PS, so leading to comparable T_g's, the η_0 value for PMMA is still 40 times as large as for PS. Fig. 11 compares the plots of complex viscosity vs. angular frequency for PS (Fig. 11a) and PMMA (Fig. 11b) of 10000 MW (thus the same MW as the PS block of Kraton D1107 and the PMMA block of MIM (sample 4)). For PMMA to have the same melt viscosity as PS, it must be heated at least 40 °C higher than PS.

The much higher zero-shear viscosity and lower M_e indicate that PMMA is less prone to flow than PS, which might explain why the MIM triblocks have to be processed at higher temperature than the SIPS analogues, consistent with a higher order-disorder transition temperature. Thus, although the T_{ODT} can be theoretically predicted[15)] from the polymer-polymer interaction parameter and the block copolymer composition, the occurrence of this transition in MIM is much delayed by unfavorable kinetic parameters.

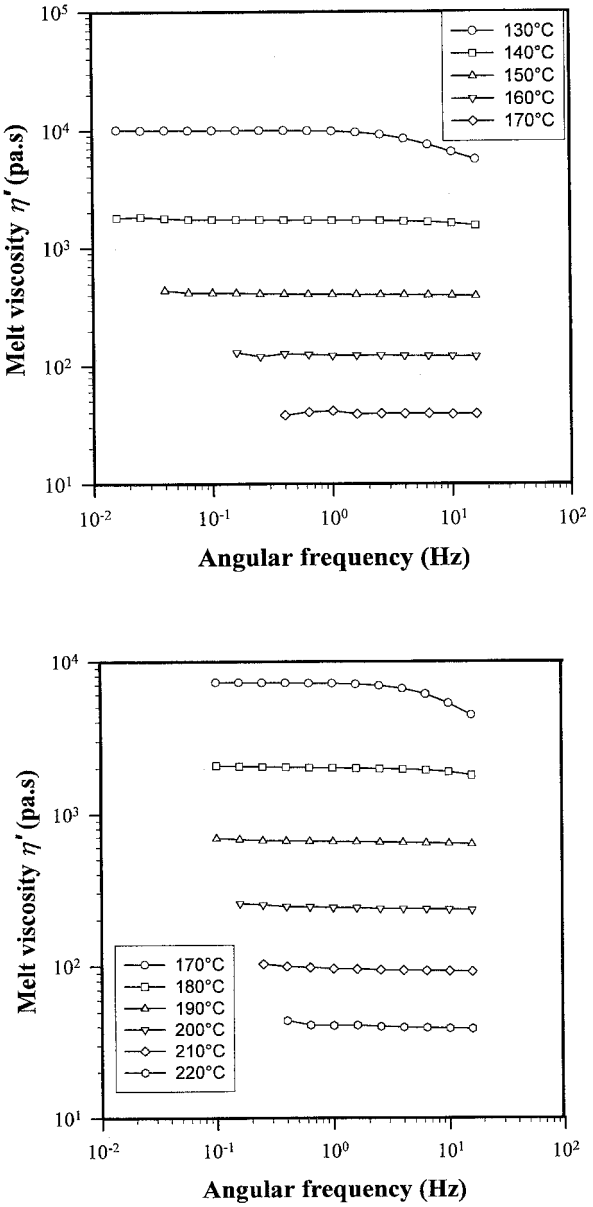

Fig. 11. Plot of melt viscosity vs. angular frequency for: (a) 10000 PS; (b) 10000 PMMA

Conclusion

The phase morphology of poly(methyl methacrylate)-*block*-poly(isooctyl acrylate)-*block*-poly(methyl methacrylate) triblock copolymers has been studied by atomic force microscopy with phase detection imaging. Spherical, cylindrical, and lamellar morphologies have been observed for block copolymers of increasing PMMA content. These copolymers exhibit a behavior typical of thermoplastic elastomers only when the PMMA molecular weight is small (3500 and 5000). Otherwise, the microdomain structure of the MIM triblocks persists beyond the glass transition temperature of PMMA. The much higher experimental T_{ODT} for MIMs compared to the SIPS analogues is not of thermodynamic origin but rather due to kinetic factors in relation to the high zero-shear viscosity and low M_e for the outer PMMA blocks.

Acknowledgements: The authors are grateful to the "*Services Fédéraux des Affaires Scientifiques, Techniques et Culturelles*" for general support in the frame of the "PAI 4/11*: Supramolecular Chemistry and Supramolecular Catalysis*". Research in Mons is also partly supported by *the European Commission and the Government of the Région Wallonne* (Project NOMAPOL-Objectif 1-Hainaut), and *the Belgian National Fund for Scientific Research* FNRS/FRFC. RL is "Maître de Recherche" by the "*Fonds National de la Recherche Scientifique*" (FNRS).

[1] R. Jérôme, J. D. Tong, *Current Opinion in Solid State and Materials Science* **3**, 573 **(**1998)
[2] R. Jérôme, Ph. Bayard, R. Fayt, Ch. Jacobs, S. Varshney, Ph. Teyssié, in: *Thermoplastic Elastomers*, 2nd edition, G. Holden, N. R. Legge, R. Quirk, H. E. Schroeder, Eds., Hanser: Munich, Vienna, New York 1999, p. 521
[3] Y. Yu, Ph. Dubois, R. Jérôme, Ph. Teyssié, *Macromolecules* **29**, 1753 and 2738 **(**1996)
[4] J. M. G. Cowie, R. Ferguson, M. D. Fernandez, M. J. Fernandez, I. J. McEwen, *Macromolecules* **25**, 3170 **(**1992)
[5] J. D. Tong, R. Jérôme, submitted for publication
[6] S. N. Magonov, M.-H. Whangbo, "*Surface Analysis with STM and AFM: Experimental and Theoretical Aspects of Image Analysis"*, VCH, Weinheim 1996, p. 39
[7] R. Soltani, F. Laupretre, L. Monnerie, Ph. Teyssié, *Polymer* **39**, 3297 **(**1998)
[8] Ph. Leclère, R. Lazzaroni, G. Moineau, M. Minet, Ph. Dubois, J. L. Brédas, R. Jérôme, submitted for publication
[9] M. A. van Dijk, R. van den Berg, *Macromolecules* **28**, 6773**(**1995)
[10] G. Bar, Y. Thomman, R. Brandsch, H. J. Cantow, M. H. Whangbo, *Langmuir* **13,** 3807 (1997); S. N. Magonov, V. Elings, W. H. Whangbo, *Surf. Sci. Lett.* **375**, L385 **(**1997); N. A. Burnham, O. P. Behrend, F. Oulevey, G. Gremaud, P.-J. Gallo, D. Gourdon, E. Dupas, A. J. Kulik, H. M. Pollock, G. A. D. Briggs, *Nanotechnology* **8**, 67 **(**1997)
[11] B. R. M. Gallot, *Adv. Polym. Sci*. **29**, 85**(**1978)
[12] G. Holden, N. R. Legge, in: *Thermoplastic Elastomers*, N. R. Legge, G. Holden, H. E. Schroeder, Eds., Hanser: Munich, Vienna, New York, 1987, p. 47
[13] D. J. Meier, *J. Polym. Sci., Part C* **26**, 81 **(**1969)
[14] E. Helfand, Z. R. Wasserman, *Macromolecules* **9**, 879 **(**1976)
[15] L. Leibler, *Macromolecules* **13**, 1062 **(**1980)
[16] F. S. Bates, G. H. Fredrickson, in: *Thermoplastic Elastomers*, 2nd ed., G. Holden, N. R. Legge, R. Quirk, H. E. Schroeder, Eds., Hanser: Munich, Vienna, New York, 1996, p. 335
[17] T. Hashimoto, in: *Thermoplastic Elastomers*, 2nd ed., G. Holden, N. R. Legge, R. Quirk, H. E. Schroeder, Eds., Hanser: Munich, Vienna, New York, 1996, p. 429
[18] C. D. Han, D. M. Baek, J. K. Kim, T. Ogawa, N. Sakamoto, T. Hashimoto, *Macromolecules* **28**, 5043 **(**1995)
[19] C. A. Berglund, K. W. Mckay, *Polym. Eng. Sci*. **33**, 1195 **(**1993)
[20] K. I. Winey, D. S. Gobran, Z. Xu, L. J. Fetters, E. L. Thomas, *Macromolecules* **27**, 2392 **(**1994)
[21] C. I. Chung, M. I. Lin, *J. Polym. Sci., Polym. Phys. Ed.* **16**, 545 **(**1978)
[22] F. S. Bates, *Macromolecules* **17**, 2607**(**1984)
[23] M. D. Gehlsen, F. S. Bates, *Macromolecules* **26**, 4122 **(**1993)
[24] R. F. Fedos, *J. Polym. Sci., Part C* **26**, 189**(**1969)
[25] H. Morawetz, *Macromolecules in Solution*, Wiley-Interscience: New York 1961, p. 41
[26] E. V. Gouinlock, R. S. Porter, *Polym. Eng. Sci.* **17**, 534 **(**1977)
[27] C. D. Han, J. Kim, *J. Polym. Sci., Part B* **25**, 1741 **(**1987)
[28] C. D. Han, D. M. Baek, J. K. Kim, *Macromolecules* **23**, 561 **(**1990)
[29] D. W. Van Krevelen, *Properties of Polymers*, 3rd Edition, Elsevier: Amsterdam, Oxford, New York, Tokyo 1990, p. 790
[30] W. M. Graessley, *Adv. Polym. Sci.* **16**, 55 **(**1974)
[31] J. L. Halary, A. K. Oultache, J. F. Louyot, B. Jasse, T. Sarraf, R. Muller, *J. Polym. Sci.*, Part B **29**, 933 **(**1991)
[32] T. Masuda, K. Kitagawa, S. Onogi, *Polym. J.* **4**, 418**(**1970)
[33] D. J. Plazek, V. Tan, V. H. O'Rourke, *Rheol. Acta* **13**, 367 **(**1974)
[34] D. J. Plazek, E. Riande, H. Markovitz, N. Ragupathi, *J. Polym. Sci., Polym. Phys. Ed.* **17**, 2189 **(**1979)
[35] S. Wu, *J. Polym. Sci., Polym. Phys. Ed.* **27**, 723 **(**1989)
[36] R. A. J. Stratton, *Coll. Interf. Sci.* **22**, 517 **(**1966)